

# Adenoviral vector saturates Akt pro-survival signaling and blocks insulin-mediated rescue of tumor-necrosis-factor-induced apoptosis

Kathryn Miller-Jensen<sup>1,2</sup>, Kevin A. Janes<sup>3</sup>, Yun-Ling Wong<sup>2</sup>, Linda G. Griffith<sup>1,3</sup> and Douglas A. Lauffenburger<sup>1,2,3,4,\*</sup>

<sup>1</sup>Biotechnology Process Engineering Center, <sup>2</sup>Department of Chemical Engineering, <sup>3</sup>Biological Engineering Division and <sup>4</sup>Department of Biology, Massachusetts Institute of Technology, Cambridge, MA 02139, USA

\*Author for correspondence (e-mail: lauffen@mit.edu)

Accepted 14 June 2006

Journal of Cell Science 119, 3788-3798 Published by The Company of Biologists 2006  
doi:10.1242/jcs.03102

## Summary

Recombinant adenoviruses are used extensively as delivery vectors in clinical gene therapy and in molecular biology, but little is known about how the viral carrier itself contributes to cellular responses. Here we show that infection with an E1/E3-deleted adenoviral vector (Adv) sensitizes human epithelial cells to tumor necrosis factor (TNF)-induced apoptosis. To explore the mechanism of Adv-mediated sensitization, we measured activity time courses for three protein kinases (MK2, IKK and JNK1) centrally involved in the TNF-receptor signaling network, as well as two kinases (Akt and ERK) activated by growth factors. Both the pro-apoptotic signal MK2 and the anti-apoptotic signal Akt were upregulated when Adv-infected cells were stimulated with TNF, and MK2 and Akt each contributed significantly to TNF-induced cell fate. Surprisingly, further activation of Akt in Adv-infected cells via insulin treatment did not significantly reduce apoptosis or MK2 activity. We show that the ineffectiveness of

insulin-mediated anti-apoptotic signaling through Akt is due to saturation of Akt-effector substrate phosphorylation in Adv-infected cells. Normalizing Akt signaling relative to its Adv-induced baseline activity identified a global dose-response curve that relates Akt signaling to cellular survival. Thus, the background Akt activity induced by Adv limits the transmission of anti-apoptotic signals in response to further cytokine or growth-factor stimulation. The phenotypic and intracellular synergy between Adv and TNF may have implications for interpreting cellular responses in gene-therapy and laboratory applications.

Supplementary material available online at  
<http://jcs.biologists.org/cgi/content/full/119/18/3788/DC1>

Key words: Adenoviral vector, Akt, Tumor necrosis factor, Insulin, Signaling

## Introduction

Recombinant adenoviruses are commonly used as delivery vectors in gene-therapy clinical trials and in basic bioscience studies for the delivery of transgenes. In both of these areas, it is important to understand how the adenoviral vector (Adv) alters cells during infection. Adv-induced cellular changes might synergize or antagonize the effects of certain transgenes, confounding interpretation of their normal role in cells. Deconstructing the contributions of Adv and the transgene is also relevant in vivo, because gene products intrinsic to Adv may cause host cells to react differently to proinflammatory cytokines that circulate during infection (Janeway, Jr and Medzhitov, 2002). The virology of wild-type adenovirus has been studied extensively (Prem, 1999), but there is not the same molecular-level understanding of the engineered Advs used in gene-therapy applications.

Adv delivery systems comprise 25% of all past and current gene-therapy clinical trials<sup>†</sup>. Most of these vectors are deleted for the adenoviral early regions E1 and E3. Despite these modifications, E1/E3-deleted Advs are not biologically inert.

Cells infected with E1/E3-deleted Adv still express low levels of other wild-type gene products, which are known to cause potent immunogenic responses (Thomas et al., 2003). These Adv gene products – especially early region E4 – along with the Adv capsid, may also modulate cellular responses (Tauber and Dobner, 2001). Although the development of helper-dependent Advs (devoid of all viral genes) continues to progress (Palmer and Ng, 2005), to date this type of vector has been used only once in a clinical trial<sup>†</sup>. It is therefore important to study cytokine-induced cell signaling networks in the context of Adv infection, including background transcription of the Adv genetic backbone.

The inflammatory cytokine, tumor necrosis factor (TNF), plays a key role in the early innate immune response and subsequent elimination of E1/E3-deleted Adv from the host (Elkon et al., 1997; Lieber et al., 1997; Zhang et al., 1998). Resident macrophages efficiently take up Advs and then release TNF within the tissue to eliminate infected cells (Lieber et al., 1998; Lieber et al., 1997). Wild-type E1 and E3 adenoviral early proteins are known to manipulate cell responses to TNF-family cytokines (Benedict et al., 2001; Duerksen-Hughes et al., 1989; Rao et al., 1992; Schaack et al., 2004). Adenoviruses normally use these E1/E3-mediated

<sup>†</sup>Genetic Modification Clinical Research Information System, <http://www.gemcris.od.nih.gov>.

mechanisms to promote cell survival long enough to complete the viral replication cycle. By contrast, how gene-therapy vectors deleted of the E1 and E3 genes alter the host-cell response to TNF-family cytokines has been largely unexplored.

Host responses to TNF are controlled by a complex intracellular signaling network of kinases, proteases and transcription factors (Wajant et al., 2003). Key pathways in the network include nuclear factor- $\kappa$ B (NF- $\kappa$ B) (Aggarwal, 2003), p38 mitogen-activated protein kinase (p38), c-Jun N-terminal kinase (JNK) (Shaulian and Karin, 2002), extracellular-regulated kinase (ERK), and Akt (Lawlor and Alessi, 2001). Many of these pathways are exploited by Adv during infection. In vitro analyses of Adv infections in several epithelial cell lines have shown that ERK (Bruder and Kovcsdi, 1997; Tamanini et al., 2003; Tibbles et al., 2002), NF- $\kappa$ B (Borgland et al., 2000; Bowen et al., 2002; Tibbles et al., 2002), p38 (Tamanini et al., 2003; Tibbles et al., 2002), and JNK (Tamanini et al., 2003) play roles in the Adv-induced early inflammatory response. In addition, the Adv protein E4 selectively activates the Akt pathway (O'Shea et al., 2005; Zhang et al., 2004). Based on the overlap in the signaling networks activated by TNF and Adv infection, we hypothesized that Adv would alter signaling and cell-fate responses to TNF. If true, this finding would have important implications for interpreting both gene-therapy and basic-bioscience studies in which Adv and TNF are involved.

Although Adv-TNF research is limited, there is extensive knowledge on crosstalk between TNF and other cytokines. For example, the immunostimulatory cytokine interferon- $\gamma$  (IFN $\gamma$ ) synergizes with TNF to promote apoptosis in tumor cell lines normally resistant to TNF-induced cell death (Fransen et al., 1986; Fulda and Debatin, 2002). By contrast, mitogenic cytokines such as insulin and epidermal growth factor (EGF) antagonize TNF-induced cell death in many cell types (Garcia-Lloret et al., 1996; Janes et al., 2006; Qian et al., 2001). It is also important to understand how Adv might alter signaling between TNF and these antagonizing growth factors.

Here we show that Adv infection dramatically sensitizes multiple epithelial cell lines to TNF-induced apoptosis. Both pro-apoptotic MK2 and anti-apoptotic Akt are upregulated in Adv-infected cells following TNF treatment. Further increases in Akt activity via the growth factor insulin do not rescue cells from TNF-induced apoptosis or lower MK2 activity. We find that loss of insulin-mediated anti-apoptotic signaling is directly linked to the high background levels of Akt activity induced by Adv, which saturates downstream Akt-effector signaling. Saturation of Akt function becomes evident when TNF-induced signaling is calculated as fold activation over the baseline measurement taken before TNF stimulation but after Adv infection. This normalization compresses both Adv-infected and IFN $\gamma$ -sensitized cells onto a single Akt-survival dose-response curve. We conclude that E1/E3-deleted Adv can generate significant alterations in key signaling pathways that fundamentally change subsequent cell responses to TNF and insulin.

## Results

### Adv-mediated sensitization of human epithelial cells to TNF-induced apoptosis

We developed a simple protocol to quantify the extent to which Adv infection alters the cell-death response to

TNF stimulation. We infected HT-29 human colon adenocarcinoma cells with either an E1/E3-deleted adenovirus carrying the CMV promoter and a  $\beta$ -gal reporter gene (Adv. $\beta$ -gal) or an identical vector without a reporter gene (Adv.empty). The final Adv concentration in the infection media was  $1.4 \times 10^{10}$  viral particles (v.p.)/ml, resulting in >95% of the cell population positive for Adv infection (data not shown). For control cells, buffer without Adv was added. TNF (100 ng/ml) was added 24 hours after the start of infection. Cells were collected 48 hours after TNF treatment and apoptosis was quantified by flow cytometry with an anti-cleaved caspase 3 antibody and the M30 antibody (Leers et al., 1999) against caspase-cleaved cytokeratin or with annexin V and propidium iodide (PI) staining (Fig. 1A,B). Adv infection alone caused only low levels of apoptosis compared with control cells; however, both assays showed that the apoptotic population significantly increased two- to threefold upon TNF-treatment in Adv-infected cells compared with that in uninfected cells ( $P < 0.01$ ; Fig. 1A). Adv constructs with and without a  $\beta$ -gal reporter enzyme resulted in similar rates of cell death, indicating that the presence of the  $\beta$ -gal transgene did not influence Adv sensitization. Furthermore, TNF-induced apoptosis required Adv preinfection in these cells, because TNF treatment by itself caused minimal cell death (Fig. 1B). Two-way ANOVA revealed a significant interaction effect between Adv infection and TNF treatment ( $P < 10^{-4}$ ), indicating that Adv infection synergistically enhances TNF-induced apoptosis in HT-29 cells.

It was possible that the high Adv titers used in the sensitization experiments had exceeded a threshold above which apoptosis occurred non-physiologically. Therefore, we explored how Adv sensitization varied with Adv dosage. Many variables affect net Adv dosage, including differences in cell-plating density, infection time, and concentration-dependent rates of diffusion (Mittereder et al., 1996; Nyberg-Hoffman et al., 1997). Here, we altered total viral uptake by changing infection time and concentration (see Materials and Methods for details). Quantitative PCR of the Adv genome revealed that TNF-mediated apoptosis correlated linearly with dosage from 0-1400 total Adv copies per cell (Fig. 1C;  $r = 0.95$ ). Viral uptake was the main contributor to sensitization, because the same linear dose dependence was observed for two different Adv concentrations, and the extent of apoptosis was unaffected when the timing between Adv removal and TNF stimulation was varied from 12-21 hours (supplementary material Fig. S1). Importantly, synergistic apoptosis was evident with as few as 400 Adv copies per cell. Since high infectivity levels are necessary to achieve efficient infection in vivo (Mizuguchi and Hayakawa, 2004), this argues that Adv sensitization to TNF-induced apoptosis can occur at clinically relevant infectivities.

To determine whether Adv-TNF synergy existed in diverse tissue types, we compared the sensitization of HT-29 cells to that of HeLa cells over a range of infectivities (MOI: 50-1000). Sensitization in both cell types increased with Adv dosage (Fig. 1D), and Adv-infected HeLa cells were actually more sensitive to TNF-induced apoptosis than HT-29 cells were. HeLa cell death after 24 hours of TNF exposure was consistently twofold greater than HT-29 cell death after 48 hours of TNF exposure. Similar dose-dependent sensitization was also observed in C3A human hepatocarcinoma cells and

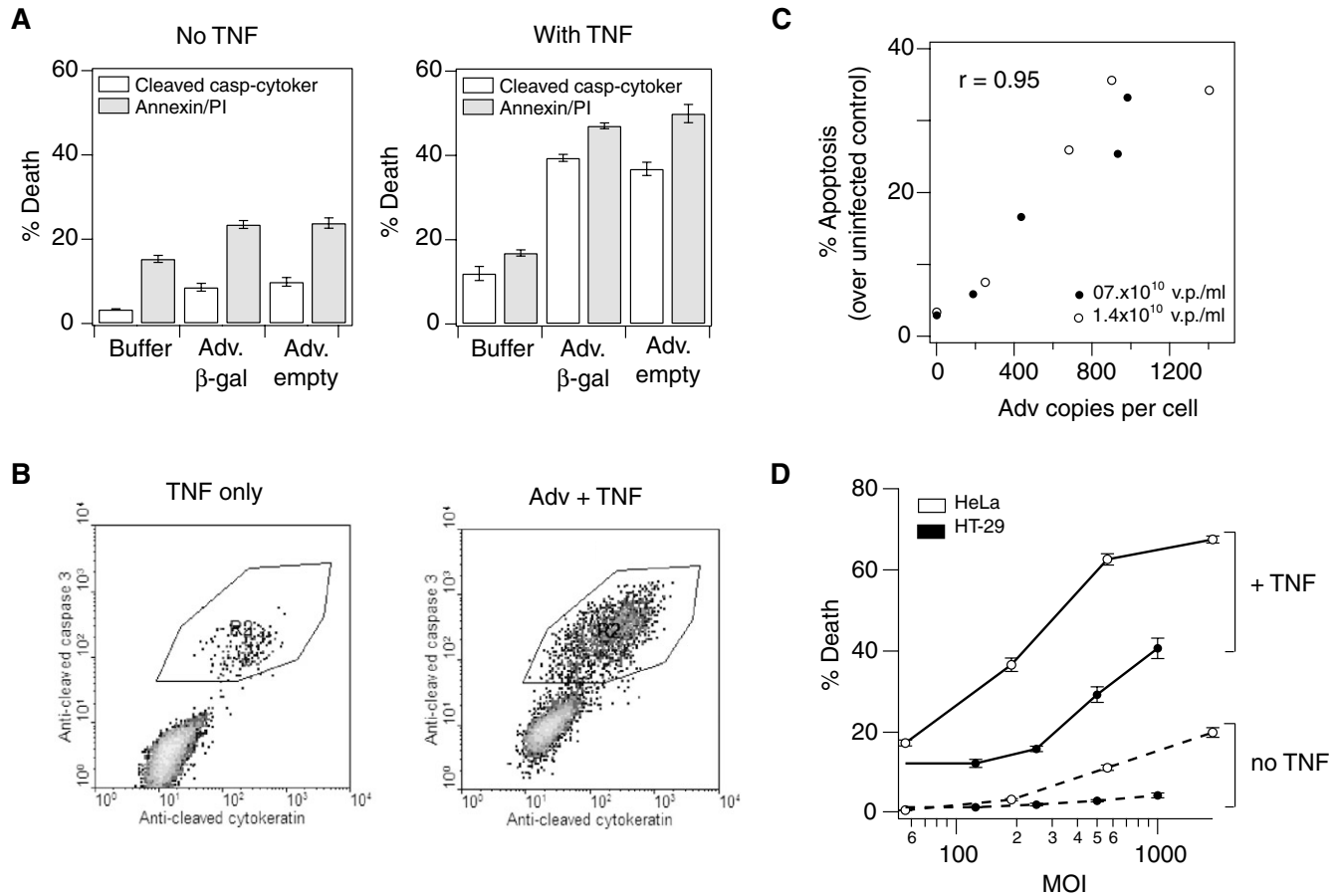


**Fig. 1.** Adv infection sensitizes human epithelial cells to TNF-mediated apoptosis. (A) HT-29 cells were infected with either Adv.β-gal or Adv.empty ( $1.4 \times 10^{10}$  v.p./ml) or treated with buffer only and then stimulated with either 100 ng/ml TNF or carrier only. Cells were collected 48 hours after TNF addition, stained for either caspase-cleaved cytokeratin and cleaved (active) caspase 3 (white bars) or annexin V/PI (gray bars), and analyzed by flow cytometry. Adv.β-gal was used for all subsequent experiments. (B) Sample flow cytometry plots for anti-caspase-cleaved cytokeratin and anti-cleaved (active) caspase 3 in Adv-sensitized and control cells treated with TNF. (C) HT-29 cells were infected with two concentrations of Adv ( $0.7 \times 10^{10}$  and  $1.4 \times 10^{10}$  v.p./ml) for 0, 1, 6 and 12 hours. The total number of Adv copies per cell was quantified by PCR. Values represent mean total β-gal DNA normalized to mean total β-actin DNA for duplicate samples. Variance in the Adv copy values ranged from 10 to 30% of the mean value. In parallel, HT-29 cells subject to the same infection conditions were treated with 100 ng/ml TNF and collected after 48 hours. Cleaved caspase 3-cytokeratin measurements are plotted as the mean apoptosis (above control level) of three biological replicates. (D) HeLa cells and HT-29 cells were infected with increasing doses of Adv (expressed as multiplicities of infection, p.f.u./cell) and stimulated with TNF or carrier, similar to panel A. Cells were collected 24 hours (HeLa) or 48 hours (HT-29) post-TNF treatment. Cleaved caspase 3-cytokeratin measurements are plotted as the mean of three biological replicates  $\pm$  s.e.m.

A549 human lung carcinoma cells (supplementary material Fig. S2). These results demonstrate that Adv synergizes with TNF to induce apoptosis in many human cell types.

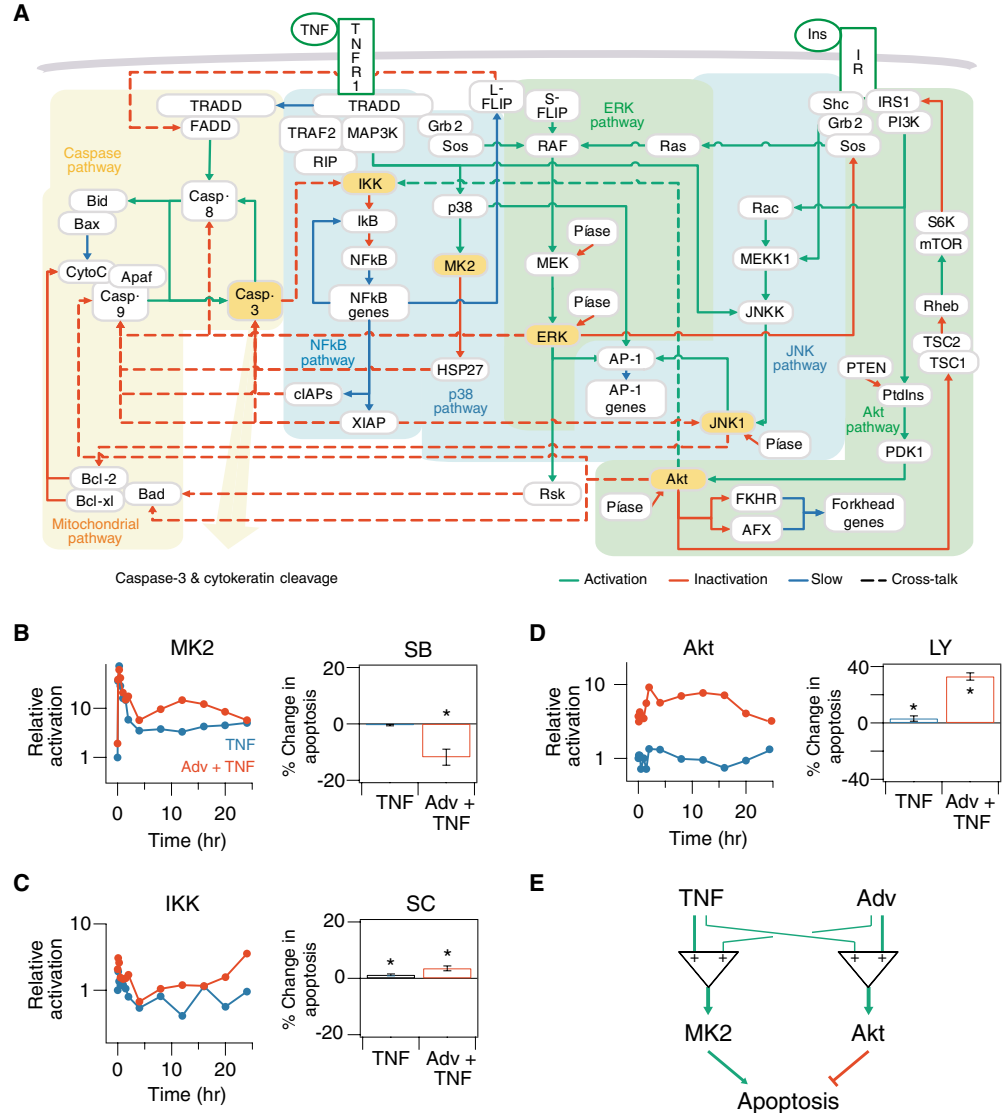
#### Adv modification of the TNF-induced signaling network

Because Adv infection sensitizes cells to TNF-induced apoptosis, we reasoned that Adv might modulate one or more kinase signaling pathways centrally involved in the TNF-activated network (Fig. 2A). Cell-death responses to TNF are highly regulated by a number of stress and survival kinases (Cowan and Storey, 2003; Hersey and Zhang, 2003; Stupack and Chersesh, 2002). In addition, Adv E4 is known to mimic growth-factor signaling, leading to activation of PI3K and Akt (O'Shea et al., 2005; Zhang et al., 2004). Therefore, we measured three kinases – MK2 (a p38 substrate), IKK and JNK1 – that are distributed within the TNF signaling network

(Fig. 2A, blue shading) as well as two growth-factor activated signals (Akt and ERK; Fig. 2A, green shading). To measure Adv-induced activity changes leading to sensitization, we treated Adv-infected and uninfected HT-29 cells with TNF (100 ng/ml) and collected cell lysates at 13 time points over 24 hours. From these cell extracts, we measured MK2, IKK, JNK1, Akt and ERK activities by using a high-throughput quantitative multiplex kinase assay (Janes et al., 2003) (supplementary material Table S1 and S2). To account for the contribution of Adv infection alone, kinase activities were also measured in Adv-infected cells after mock stimulation (supplementary material Table S3). Finally, to determine the phenotypic consequences of each kinase activity, we measured the change in TNF-stimulated apoptosis in the presence of pathway-specific, small-molecule inhibitors.

We observed potent activation of the TNF signaling network

**Fig. 2.** Adv infection upregulates TNF-induced pro- and anti-apoptotic signaling. (A) The signaling pathways induced by TNF (blue) and insulin (green). The kinases measured (MK2, IKK, JNK1, Akt and ERK) are highlighted in yellow. Figure is modified and published with permission from the American Society for Biochemistry and Molecular Biology (Gaudet et al., 2005). (B-D) Dynamic activation status and inhibitor response data for the MK2 pathway (B), IKK pathway (C) and Akt pathway (D) in uninfected cells treated with 100 ng/ml TNF (TNF; blue) and Adv-infected cells treated with 100 ng/ml TNF (Adv + TNF; red). Lysates were collected at 0, 5, 15, 30, 60 and 90 minutes and 2, 4, 8, 12, 16, 20 and 24 hours, and kinase activity was measured by a high throughput kinase activity assay and normalized to total protein content. Results are plotted as the mean relative activation of two biological replicates normalized to activity of the untreated control at 0 minutes (i.e. uninfected cells). The significance of the difference between each pair of curves was calculated by two-way ANOVA (MK2:  $P < 0.01$ ; IKK:  $P < 0.001$ ; Akt:  $P < 10^{-4}$ ). Apoptosis in the presence of kinase inhibition was measured by flow cytometry for cleaved caspase-cytokeratin. The following inhibitor concentrations were used: 10  $\mu$ M SB202190 (SB); 20  $\mu$ M SC-514 (SC); 20  $\mu$ M LY294002 (LY). Cells were collected at 24 hours, rather than 48 hours, to minimize baseline apoptosis resulting from inhibition. Measurements are plotted as the mean percentage change in apoptosis resulting from inhibition (i.e. mean percentage apoptosis in the presence of inhibitor – mean percentage apoptosis without inhibitor) of three (SC) or six (SB, LY) biological replicates  $\pm$  s.e.m. Note that LY plot ranges from  $-40$  to  $+40$  (compared with  $-20$  to  $+20$  for other inhibitor plots). Changes are labeled as significant (\*) if  $P < 0.05$ . (E) Adv-TNF synergy via pro-apoptotic p38-MK2 signaling and anti-apoptotic PI3K-Akt signaling. Synergy is illustrated schematically as an operational amplifier, with the strength of the Adv or TNF input into either the MK2 or Akt signaling time-course indicated by line weight. Amplification of the inputs results in activation (MK2) or inhibition (Akt) of apoptosis.



when either uninfected or Adv-infected cells were treated with TNF (Fig. 2B,C and supplementary material Fig. S3A). Among TNF pathways, Adv infection significantly increased TNF-induced MK2 and IKK signaling ( $P < 0.01$ , two-way ANOVA; Fig. 2B,C) but not JNK1 ( $P = 0.71$ ; supplementary material Fig. S3A). These altered intracellular patterns were a product of Adv-TNF synergy, because Adv infection alone contributed minimally to JNK1, IKK and MK2 activation (supplementary material Fig. S4A). Small-molecule inhibition of the measured pathways confirmed the importance of MK2 and IKK for Adv sensitization. Inhibition of the upstream activator of MK2 with the highly specific inhibitor SB202190 (Davies et al., 2000) significantly decreased apoptosis ( $P < 0.01$ ), suggesting a pro-apoptotic role. Conversely, IKK inhibition with SC-514 resulted

in a small but significant increase in apoptosis ( $P < 0.05$ ), consistent with the recognized anti-apoptotic functions of IKK (Karin and Ben-Neriah, 2000). We confirmed this result with the mechanistically distinct inhibitor peptide, SN50 (supplementary material Fig. S5A). JNK1 was transiently activated by TNF but was unchanged by Adv infection; thus, as expected, JNK1 inhibition with SP600125 did not significantly affect Adv-sensitized cell death (supplementary material Fig. S3A). We conclude that, of the TNF-dependent kinases measured, the p38-MK2 pathway is the most important pro-apoptotic signal contributing to Adv-TNF synergy.

Both growth-factor pathways were also strongly activated by Adv and TNF (Fig. 2D and supplementary material Fig. S3B). Similarly to TNF-induced JNK1, ERK was transiently activated

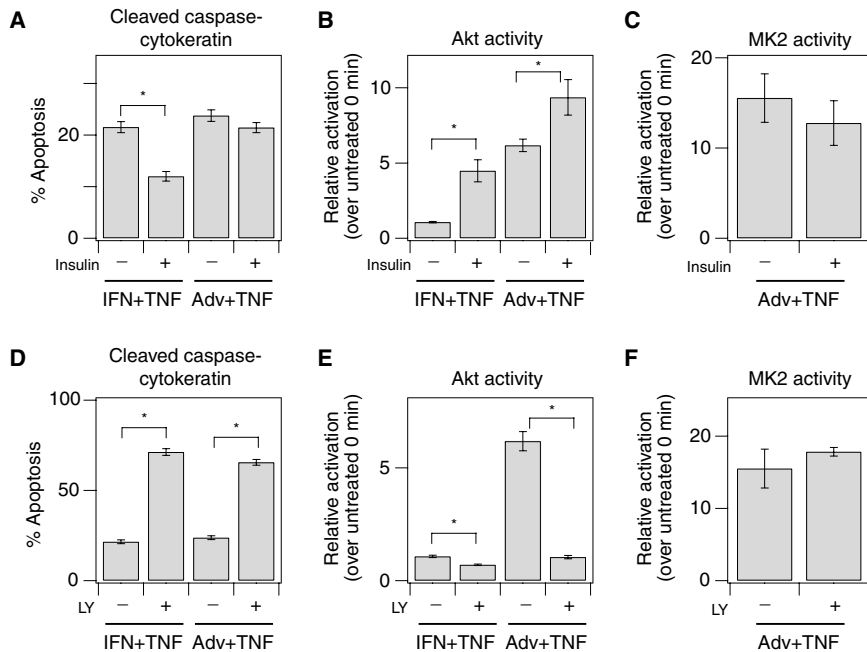


**Fig. 3.** Insulin increases Akt activity but does not reverse TNF-induced apoptosis or reduce MK2 activity in Adv-infected cells. Adv- and IFN $\gamma$ -sensitized HT-29 cells were treated with TNF (100 ng/ml and 50 ng/ml, respectively) in the presence and absence of (A-C) 100 nM insulin or (D-F) 20  $\mu$ M LY294002. Cells were lysed at 12 hours and assayed for kinase activity, or collected after 24 hours and assayed for apoptosis by flow cytometry for cleaved caspase-cytokeratin. (A,D) Change in TNF-induced cell death. Measurements are plotted as the mean of six biological replicates (two independent experiments)  $\pm$  s.e.m. (B,E) change in TNF-induced Akt activity. Measurements are plotted as the mean of six biological replicates (two independent experiments)  $\pm$  s.e.m. (C,F) Change in TNF-induced MK2 activity in Adv-sensitized cells. Measurements are plotted as the mean of three biological replicates  $\pm$  s.e.m. Changes are labeled as significant (\*) if  $P < 0.05$ .

by TNF but was not differentially affected by prior Adv infection. Thus, inhibition of the upstream ERK kinase with U0126 did not significantly affect Adv-TNF synergy (supplementary material Fig. S3B). By contrast, Adv infection alone induced a three- to fivefold increase in Akt activity for up to 24 hours ( $P < 0.01$ ; supplementary material Fig. S4B), consistent with the PI3K-activating role of E4 (O'Shea et al., 2005; Zhang et al., 2004). Akt activation was further increased by TNF treatment, resulting in eight- to tenfold greater activity than in uninfected TNF-treated cells ( $P < 10^{-10}$ ; Fig. 2D). Akt transmits many key pro-survival signals (Lawlor and Alessi, 2001), and we found that upstream PI3K inhibition with LY294002 dramatically increased synergistic apoptosis mediated by Adv and TNF ( $P < 10^{-4}$ ). We found a similar result with the mechanistically distinct inhibitor, wortmannin (supplementary material Fig. S5B). Together, these experiments indicate that Adv infection synergizes with TNF by augmenting an existing p38-MK2 pro-death signal and adding a new PI3K-Akt pro-survival signal that is then further activated by TNF (Fig. 2E).

#### Upregulation of endogenous Akt activity in Adv-infected cells by insulin

Despite potent Akt signaling in Adv-infected cells (Fig. 2D), synergistic apoptosis still occurred after TNF stimulation (Fig. 1). The LY294002 inhibitor experiment confirmed a pro-survival role of Akt by downregulation (Fig. 2D). However, the contribution of some pro-survival molecules has been shown to vary depending upon whether protein function is increased or decreased (Hua et al., 2005). To activate endogenous Akt, we therefore used the growth factor insulin, which is reasonably specific in its activation of Akt in HT-29 cells (Gaudet et al., 2005). Additionally, insulin is known to inhibit TNF-induced cell death (Remacle-Bonnet et al., 2000) through upregulation of Akt activity in HT-29 cells sensitized with IFN $\gamma$  (Janes et al., 2003). To test whether insulin similarly provides protection from TNF-induced apoptosis in HT-29

cells sensitized by Adv, we added 100 nM insulin together with TNF. In contrast to IFN $\gamma$ -sensitized cells, insulin did not decrease TNF-induced apoptosis in Adv-infected cells ( $P = 0.15$ ; Fig. 3A). Surprisingly, this was not due to a lack of Akt signaling, since insulin increased Akt activity to a similar extent in both Adv-sensitized cells and IFN $\gamma$ -treated cells ( $P < 0.05$ ; Fig. 3B). There was not a significant decrease in TNF-induced MK2 activity in Adv-infected cells as a result of insulin stimulation ( $P = 0.49$ ; Fig. 3C), confirming the selectivity of insulin as an Akt-selective agonist. To verify that IFN $\gamma$ - and Adv-sensitized cells behaved similarly when Akt was inhibited, we measured TNF-induced apoptosis and Akt activity in the presence of LY294002. For both sensitizing agents, LY294002 inhibition significantly increased TNF-induced apoptosis ( $P < 10^{-9}$ ; Fig. 3D) and reduced Akt activity ( $P < 0.001$ ; Fig. 3E), as expected. Again, there was no change in MK2 activity in Adv-sensitized cells as a result of Akt inhibition ( $P = 0.45$ ; Fig. 3F), indicating that MK2 pro-apoptotic signaling is separable from Akt activity changes in Adv-infected cells. The lack of apoptotic rescue shows that the insulin-induced Akt activation in Adv-infected cells does not result in functional anti-apoptotic signaling.

#### Saturation of downstream Akt effectors by Adv

The lack of pro-survival signaling by insulin-mediated Akt activation could be explained by an inability to phosphorylate downstream Akt effectors in Adv-infected cells. To test this, we measured phosphorylation levels of multiple Akt substrates in Adv- and IFN $\gamma$ -sensitized HT-29 cells after TNF stimulation alone and in the presence of LY294002 or insulin. We used an Akt-phosphosubstrate (Akt-pSub) antibody that binds specifically to phosphorylated substrates of Ser/Thr kinases that recognize the RxRxxS/T motif (Manning et al., 2002). In addition, we measured levels of phosphorylated glycogen synthase kinase-3 $\alpha$  and  $\beta$  (pGSK-3 $\alpha/\beta$ ), an established substrate of Akt (Cross et al., 1995). Western blotting of HT-29 lysates showed that pGSK-3 $\alpha/\beta$  and multiple Akt-pSubs

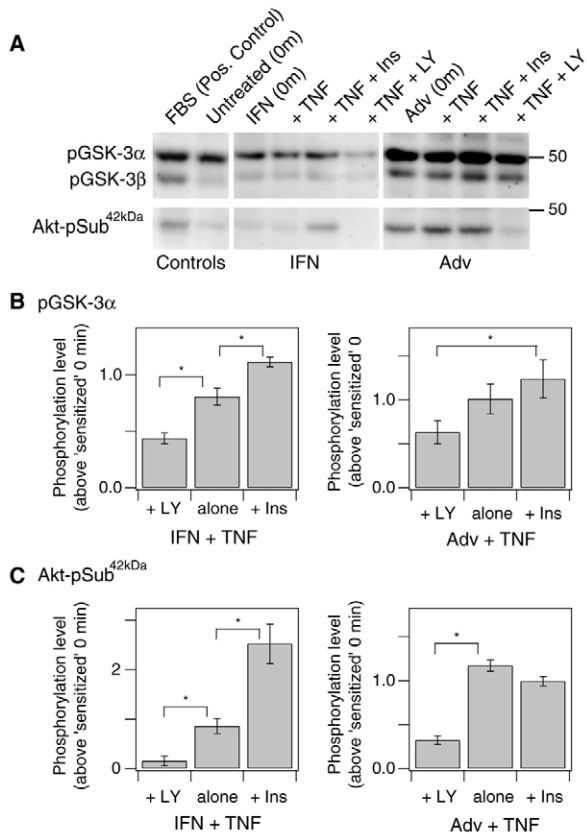


**Fig. 4.** Adv infection saturates phosphorylation of downstream Akt effectors. (A) Cells were treated as described in Fig. 3, lysed at 12 hours and analyzed by western blot by probing with anti-pGSK-3 $\alpha$ / $\beta$  and anti-Akt-pSub. Experimental conditions are the same as those described in Fig. 3. 10% fetal bovine serum (FBS) stimulation for 15 minutes was used as the positive-control stimulus. 50  $\mu$ g protein was loaded into each lane. (B,C) Adv-sensitized and IFN $\gamma$ -sensitized (B) pGSK-3 $\alpha$  and (C) Akt-pSub<sup>42kDa</sup> bands were quantified by densitometry and normalized to the sensitized (Adv or IFN $\gamma$ ) 0-min band. Measurements are plotted as the mean of three biological replicates  $\pm$  s.e.m. Changes are labeled as significant (\*) if  $P < 0.05$ .

were significantly upregulated in Adv-sensitized cells compared with IFN $\gamma$ -sensitized and untreated cells, even before the addition of TNF (Fig. 4A and supplementary material Fig. S6). This is consistent with the high baseline Akt activity induced by Adv (Fig. 2D). Two Akt-inducible proteins, pGSK-3 $\alpha$  and Akt-pSub<sup>42kDa</sup> (Fig. 4A), were quantified by densitometry and normalized to the Adv- or IFN $\gamma$ -sensitized zero-minute band. For both IFN $\gamma$  and Adv pretreatments, TNF-inducible phosphorylation of GSK-3 $\alpha$  and Akt-pSub<sup>42kDa</sup> was reduced with LY294002 treatment (Fig. 4B,C), confirming that both proteins are reliable indicators of functional Akt activity. In IFN $\gamma$ -TNF-treated cells, insulin significantly increased pGSK-3 $\alpha$  and Akt-pSub<sup>42kDa</sup>, but there was no significant insulin-induced phosphorylation of these proteins in Adv-TNF-treated cells, despite clear insulin-induced activation of Akt in Adv-infected cells (Fig. 3B). Thus, Akt activation in Adv-infected cells sustains phosphorylation of downstream effectors, but further Akt activation induced by insulin fails to increase Akt-effector phosphorylation. We conclude that Adv

infection in combination with TNF saturates the ability of Akt to phosphorylate its substrates, contributing to the observed loss of insulin-mediated anti-apoptotic signaling.

**Construction of a global Akt-survival dose-response curve combining Adv- and IFN $\gamma$ -mediated sensitization**  
 Insulin caused a similar absolute increase in Akt signaling in both IFN $\gamma$ -sensitized and Adv-infected cells, adding roughly three Akt-activity units at 12 hours after stimulation (Fig. 3B). However, relative to the baseline Akt signal induced by each pretreatment before TNF stimulation (0-min time point), the ‘fold activation’ of Akt induced by insulin was larger for IFN $\gamma$ -sensitized cells (3.7-fold) than for cells infected with Adv (2-fold; supplementary material Fig. S7). Recently, it has been suggested that cells become quickly desensitized to absolute levels of signaling and are often more responsive to gradients of signals (Sasagawa et al., 2005). To examine the importance of fold changes, we measured Akt activity and TNF-induced apoptosis under a set of Adv, IFN $\gamma$ , LY, and insulin conditions that gave a range of TNF-induced apoptotic responses (see Fig. 5 legend and Materials and Methods). Then, we preprocessed the data by normalizing IFN $\gamma$ - and Adv-sensitized cells to their respective zero-minute values to calculate ‘fold activation’ (see Materials and Methods; supplementary material Table S4). When cell viability was plotted against this fold activation of Akt, we found that both IFN $\gamma$ -TNF and Adv-TNF treatments collapsed onto a common sigmoidal dose-response curve (Fig. 5A). Preprocessing measurements of Akt-effector substrates in the same manner resulted in a dose-response identical to that of Akt, with the exception of a twofold faster transition steepness between minimum- and maximum-observed viability (Fig. 5B). The faster viability transition for Akt-effector substrates is consistent with the known ultrasensitivity that arises from sequential signaling cascades (Goldbeter and Koshland, Jr, 1984). The existence of a single function – relating fold activation of the PI3K-Akt pathway to viability for a wide range of treatment conditions – suggests that the relative change in Akt signaling is more important than its absolute level for determining TNF-induced cell fate.

The calculated Akt-survival dose-response provides a quantitative explanation for how insulin is unable to attenuate synergistic TNF-induced apoptosis in Adv-infected cells (Fig. 3A). First, by dramatically increasing the baseline Akt signal (supplementary material Fig. S7), Adv infection reduces insulin’s ability to induce a strong fold activation of the PI3K-Akt pathway (Fig. 3B). This prevents Adv-infected cells from moving far rightward on the dose-response curve in Fig. 5A. Second, our panel of experimental treatments indicates that the role of Akt signaling in these cells is most apparent when pathway activity is reduced to levels that are below baseline signaling. Adv-infected cells are thus positioned very near the upper viability-plateau of the dose-response (Fig. 5A, condition 6), suggesting a limited capacity to reduce TNF-induced apoptosis further. Together, this indicates that Adv infection traps cells in a network state that prevents insulin from transmitting additional anti-apoptotic information via the Akt pathway.

## Discussion

Our aim in this study was to explore how Adv alters human epithelial-cell signaling and apoptotic responses to the

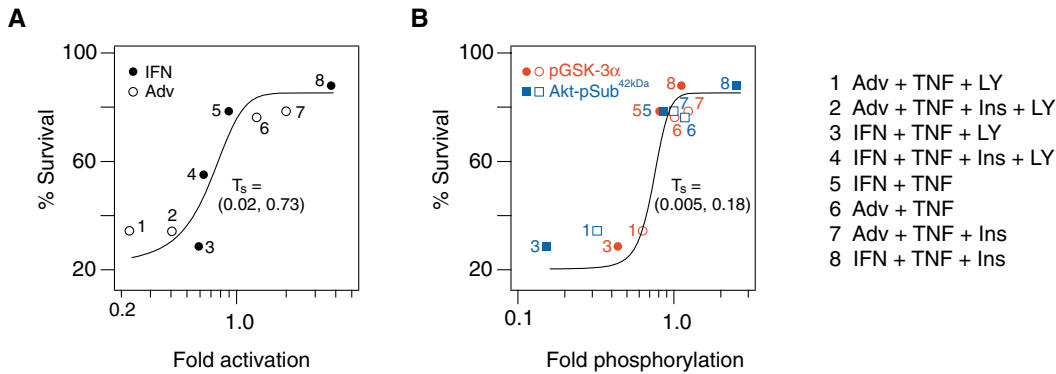


**Fig. 5.** Adv-infected are trapped near the plateau of a global Akt-survival dose-response curve. (A,B) Following Adv or IFN $\gamma$  sensitization, cells were treated with TNF (100 ng/ml and 50 ng/ml, respectively), TNF + LY294002 (20  $\mu$ M), TNF + insulin (100 nM), or TNF + LY294002 + insulin (B only). Conditions were chosen to generate a range of Akt activities. Measurements were taken at 12 hours for Akt activity and effector phosphorylation and at 24 hours for apoptosis as described in Fig. 3. (A) Cell survival versus fold activation of Akt activity. Akt activities were normalized to sensitized 0-min values from A. Akt measurements are the mean of six biological replicates. Survival measurements are 100% – the mean of six biological replicates. (B) Plot of survival (from A) versus effector phosphorylation levels quantified in Fig. 4. Solid red markers indicate IFN $\gamma$ -sensitized conditions and open red markers indicate Adv-sensitized conditions (same as in A). (A,B) Sigmoid function and parameters were calculated as described in Materials and Methods. Transition steepness ( $T_s$ ) and the upper and lower bounds of the 90% confidence interval (parentheses) are labeled on the graphs.

inflammatory cytokine TNF. Compared with wild-type adenovirus, there are relatively few studies on Adv infection and its interaction with host-cell signaling pathways. Understanding how Adv-infected cells respond in the context of a cytokine-rich environment, such as an inflamed tissue, is critical to improving gene-therapy applications. MOIs at the injection site can be very high *in vivo* (Mizuguchi and Hayakawa, 2004), similar to the ratios used in this study. High concentrations of Adv *in vivo* activate innate immune responses independent of viral gene transcription (Muruve et al., 1999; Schnell et al., 2001; Zhang et al., 2001). Neutrophils, natural killer cells, and macrophages are recruited to the site of infection where they secrete cytokines such as TNF. TNF and TNF-family cytokines are directly responsible for apoptosis in the target cells (Muruve et al., 1999; Zhang et al., 2002). Adv infection, immune-cell activation, cytokine release, and host-cell death are complex, overlapping events *in vivo*. By studying Adv infection and apoptosis in the context of one defined cytokine *in vitro*, we were able to discover that Adv and TNF cooperate to promote cell death in infected cells. Adv-TNF synergy could be an important contributor to gene-therapy side-effects, which have been reported in non-human primates studies and in Adv clinical trials (Lozier et al., 2002; Morral et al., 2002; Raper et al., 2002).

E1/E3-deleted Advs are commonly used in laboratory experiments as delivery vectors to overexpress or inhibit pathways and elucidate function. Such studies assume that changes caused by Adv infection and changes caused by the transgene are linearly cumulative. If true, then infection with an Adv that lacks the transgene is an adequate control. However, the results here show that Adv itself can significantly alter signaling pathways in the cell, both at the basal level (e.g. Akt) and in response to TNF (e.g. MK2). For Adv and TNF, cell response to Adv and TNF is highly non-linear, with the underlying impact of infection becoming apparent only after cytokine stimulation. This reveals an important caveat for interpreting laboratory studies involving Adv. Controls with

'empty' Adv might well be complemented by delivering the transgene (and associated control) with a different vector, such as liposomes for transient expression and lentiviruses or adeno-associated viruses for stable expression.

Adv-TNF synergy could also be exploited to design Advs for cancer gene therapy, for instance by delivering a TNF-family cytokine as a transgene (Armeanu et al., 2003; Griffith et al., 2000; Rasmussen et al., 2002; Voelkel-Johnson et al., 2002). Many tumors are resistant to TNF-induced apoptosis (Fransen et al., 1986), but presentation in the context of Adv infection can induce apoptosis in multiple carcinomas (Armeanu et al., 2003; Voelkel-Johnson et al., 2002). The results presented here argue that the efficacy of these cancer gene therapy approaches is a direct product of Adv-TNF synergy. An important consideration for cancer therapies is the role of Akt in Adv-infected cells. Many tumors, especially brain, breast and prostate cancer, have constitutive Akt activity due to a loss of function mutation in the PTEN phosphatase gene (Li et al., 1997). Our model suggests that Adv-mediated gene transfer may serve as an even more potent pro-death stimulus in these tumors, because the anti-apoptotic function of the Akt pathway would already be saturated before infection. Subsequent cytokine stimulation would therefore activate only pro-apoptotic signals, leading to rapid apoptosis of the tumor cells. To our knowledge, there are as yet no examples of therapies that test this prediction.

It was previously reported in the literature that Adv infection protects lung epithelial cells from TNF-induced apoptosis as a result of Adv-mediated pro-survival signaling via Akt (Flaherty et al., 2004). Notably, however, this study added actinomycin D (ActD) concurrent with TNF, thus blocking TNF transcriptional signaling. Different protein-synthesis and genetic perturbations can cause distinct mechanisms of TNF-induced apoptosis (Ventura et al., 2004). Previous work from our laboratory also suggests that information processing in cytokine-stimulated cells involves changes in gene transcription between 2 and 8 hours (Gaudet et al., 2005). MK2

activation in Adv-TNF-treated cells, which we have shown to be pro-apoptotic, has a clear second peak beginning at 4 hours (Fig. 2B). MK2 activity is important in stabilization of many proinflammatory-cytokine transcripts (Kotlyarov et al., 1999), which would be absent in transcriptionally inhibited cells. Thus, TNF+ActD and TNF alone may activate significantly different signaling network programs, explaining the discrepancy in findings. In the absence of transcriptional inhibition, we demonstrate that Adv synergizes with TNF to induce apoptosis.

A surprising result of our work is that regimes exist where increased Akt activity produces limited pro-survival benefit. We showed that this is partly due to saturation of Akt-effector phosphorylation, but it remains unclear why saturation occurs. Saturation of the PI3K-Akt pathway has also been reported in other contexts – for instance, in response to high concentrations of certain growth factors (Park et al., 2003) – suggesting that saturation is not Adv-specific. The simplest molecular explanation for saturation in Adv-infected cells is that Akt and its substrates are negatively regulated by different protein phosphatases. Akt forms complexes with protein phosphatase 2A (PP2A) (Beaulieu et al., 2005) and a protein phosphatase 2C (PP2C) family member (Gao et al., 2005), which dephosphorylate the T308 and S473 sites on Akt. By contrast, the Akt substrate GSK-3 $\beta$  coassociates with protein phosphatase 1 (PP1) (Tanji et al., 2002), as well as a PP1 regulatory subunit (Sakashita et al., 2003), which is a recognized substrate of GSK-3 $\beta$  (Hemmings et al., 1982). Thus, PP2A and PP2C could allow Adv- and insulin-mediated activation of Akt, but PP1 may block additional phosphorylation of GSK-3 $\beta$ . Such Akt-independent control of GSK-3 $\beta$  and the closely related isoform GSK-3 $\alpha$  could be particularly important for Adv-TNF synergy and apoptosis, because GSK-3 $\beta$  signaling is important for resistance to TNF-induced cell death (Hoefflich et al., 2000).

Our results suggest several mechanisms by which Adv and TNF may synergize to induce apoptosis. One pathway we identified to be directly involved was via the stress kinase MK2. Among its substrates, MK2 directly phosphorylates small heat shock protein 27 (Hsp27), which reduces its ability to protect against oxidative stress (Rogalla et al., 1999). Reactive oxygen has recently been implicated in TNF signaling (Karin and Ben-Neriah, 2000; Ventura et al., 2004), which together is consistent with the pro-apoptotic role we observed for MK2. At the post-transcriptional level, MK2 contributes to the regulation of several cytokines, including TNF (Kotlyarov et al., 1999). Adv-TNF activation of MK2 in vivo may start a positive feedback loop in cells of the innate immune system that augments cytokine production. Adv infection may also induce secretion of interferon- $\alpha$  (IFN $\alpha$ ) in host epithelial cells. Upregulation of IFN $\alpha$  could partially inhibit protein synthesis within the cell (Goldsby et al., 2000), limiting NF- $\kappa$ B-mediated transcription of molecules, such as c-FLIP (Kreuz et al., 2001), which are activated in response to TNF and prevent apoptosis. Any attenuation of NF- $\kappa$ B signaling would need to occur downstream of IKK, because TNF-induced IKK activation was not decreased but increased after Adv infection.

One possible systems-level explanation for Adv sensitization is that IKK-NF- $\kappa$ B and PI3K-Akt collaborate via a common dose-response for survival. In this case, saturation of survival signaling by Adv-mediated upregulation of Akt

may proportionally reduce the pro-survival contribution of IKK. NF- $\kappa$ B is a recognized determinant for survival in the presence of TNF (Beg and Baltimore, 1996; Van Antwerp et al., 1996; Wang et al., 1996), but we found that small molecule inhibition of IKK did not cause a pronounced increase in TNF-induced apoptosis in Adv-sensitized cells (Fig. 2B). These data support the hypothesis that Akt activation by E4 of Adv (O'Shea et al., 2005) could saturate total pro-survival signaling from both Akt and IKK-NF- $\kappa$ B. Akt and IKK have been implicated in a common signaling pathway under certain circumstances (Ozes et al., 1999; Romashkova and Makarov, 1999) and apoptosis has been shown to be determined by combinations of multiple intracellular signaling pathways (Janes et al., 2005; Janes et al., 2004). Cooperation between Akt and IKK may therefore uncouple the contribution of IKK to TNF anti-apoptotic signaling.

Despite deletion of several immunogenic regions, gene-therapy Advs still retain some of the host cell modulators found in the original adenoviral pathogen. In epithelial cells, Adv infection is revealed at the phenotypic level by treatment with TNF. Intracellular Adv-TNF synergy was uncovered by dynamically measuring the TNF-growth factor signaling network via five key protein kinases. Further systems analyses of the synergy between Adv and proinflammatory cytokines such as TNF could aid the design of next-generation viral vectors for treating human disease (Verma and Weitzman, 2005).

## Materials and Methods

### Adenovirus vectors

The recombinant adenovirus type 5 vectors with E1 and E3 regions deleted expressing either *Escherichia coli*  $\beta$ -galactosidase ( $\beta$ -gal) under control of the cytomegalovirus (CMV) enhancer/promoter (Adv- $\beta$ -gal) or containing the CMV enhancer/promoter without a transgene (Adv.empty) were provided by the University of Michigan Vector Core. Virus was provided at a concentration of  $4 \times 10^{12}$  viral particles (v.p.) per ml and reported to have an infectious plaque-forming unit (p.f.u.) concentration of  $1.7 \times 10^{11}$  p.f.u./ml as determined by plaque assay. Working viral stocks were diluted in storage buffer (10 mM Tris-HCl pH 7.4, 137 mM NaCl, 5 mM KCl, 1 mM MgCl<sub>2</sub>, 10% glycerol). Storage buffer was also used for controls.

### Cell culture and infection

HT-29 and HeLa cells (ATCC, Manassas, VA) were grown according to the manufacturer's recommendations. Unless otherwise specified, HT-29 cells were seeded at 50,000 cells/cm<sup>2</sup>, grown for 24 hours, and then infected for 6 hours in culture media (50% of normal media volume) containing  $1.4 \times 10^{10}$  v.p./ml Adv or an equivalent volume of media containing storage buffer. At the end of the infection period, cells were washed once with PBS and a full volume of fresh culture media was replaced. Using these infection conditions,  $1.4 \times 10^{10}$  v.p./ml was the lowest concentration tested that resulted in more than 95% of the cell population positive for Adv infection (data not shown). A similar infection efficiency in HT-29 cells has been reported elsewhere (Saito et al., 2003). Therefore, we used this Adv concentration for all experiments except dose-response curves (for which concentrations are indicated in text). HeLa cells were seeded at 20,000 cells/cm<sup>2</sup> and infected as described for HT-29 cells at v.p. concentrations indicated in the text.

### Apoptosis assays

HT-29 or HeLa cells were seeded and infected as described above. 24 hours after the start of infection, TNF (Peprotech; 100 ng/ml final concentration) or an equivalent volume of carrier (50:50 DMSO:water) was added to the culture media. For inhibitor studies, inhibitor or DMSO carrier was added to the medium 1 hour before TNF stimulation and collected 24 hours later. Inhibitors (Calbiochem) used were 20  $\mu$ M LY294002, 10  $\mu$ M U106, 10  $\mu$ M SB202190, 10  $\mu$ M SP600125 and 20  $\mu$ M SC-514. For growth factor studies, cells were treated with 100 nM insulin (Sigma), in parallel with TNF treatment, and collected 24 hours after stimulation. At the indicated time, cells were rinsed with PBS and trypsinized. The supernatant and rinse were saved and combined with the trypsinized cells to ensure capture of both floating and adherent cells. The cells were washed with PBS, and either all or a portion of the cells were fixed in 100% methanol and stored at -20°C. The fixed cells were stained with a fluorescein-labeled monoclonal antibody against caspase-

cleaved cytokeratin (M30; Roche) and active cleaved caspase-3 (BD Pharmingen) with Alexa 647-conjugated anti-rabbit secondary (Molecular Probes) according to the manufacturer's instructions. Cells were washed once after staining and analyzed by flow cytometry (FACS-Calibur; Becton-Dickinson). To perform parallel apoptosis assays, a portion of the original (unfixed) sample was stained with an Alexa Fluor 488 annexin V conjugate (Molecular Probes), counterstained with propidium iodide (PI; Molecular Probes) according to the manufacturer's instructions, and analyzed by flow cytometry. In some cases, a portion of the original infected sample was used for  $\beta$ -gal activity analysis to confirm a productive infection (data not shown).

### Quantitative polymerase chain reaction (PCR)

HT-29 cells were grown in 6-well plates and infected for the indicated times in either full media volume at a concentration of  $0.7 \times 10^{10}$  v.p./ml or half volume at a concentration of  $1.4 \times 10^{10}$  v.p./ml (all samples subject to the same overall MOI of 1000 p.f.u./cell). At the end of the infection time, cells were washed with PBS and trypsinized. DNA was extracted using the DNeasy Tissue Kit (Qiagen, Valencia, CA) according to the manufacturer's instructions. Genome quantification was performed using the AbiPrism 7700 (PE Biosystems) according to the method previously reported (Varga et al., 2001) with modifications. Taqman primers and probes were used to amplify the  $\beta$ -galactosidase reporter gene, and were designed using the Primer3 software package ([http://frodo.wi.mit.edu/cgi-bin/primer3/primer3\\_www.cgi](http://frodo.wi.mit.edu/cgi-bin/primer3/primer3_www.cgi)) acquired from Applied Biosystems (PE Biosystems). The probe utilized a 3' TAMRA quencher molecule attached via a linker arm and a 5' covalently linked FAM fluorescent dye. The same Taqman primers and probe were used on known quantities of gWiz  $\beta$ -Gal plasmid standards (Aldevron) to calculate a quantitative viral copy number for each sample. Data were analyzed with an ABI Sequence Detector v1.6.3 and total  $\beta$ -galactosidase DNA was normalized to total  $\beta$ -actin DNA for each sample using primers, probes and standards from the human  $\beta$ -actin Gene kit (PE Biosystems). Results are presented as the average of total  $\beta$ -gal DNA normalized to total  $\beta$ -actin DNA.

For apoptosis measurements performed in parallel with quantitative PCR analysis, infection media was aspirated at the indicated times, cells were washed once with PBS, and fresh media was replaced. Cells were then treated with TNF, collected, and analyzed by flow cytometry as described above.

### Kinase activity assays

For kinase activity assays, HT-29 cells were grown and infected as described above. 24 hours after the start of infection, TNF was added to the culture media (100 ng/ml final concentration) for the indicated times. For Akt activity studies, 20  $\mu$ M LY294002 was added to the medium 1 hour before TNF stimulation, and 100 nM insulin was added in parallel with TNF stimulation, as indicated. Cells pretreated with IFN $\gamma$  were treated as previously described (Janes et al., 2003). Cell lysates were prepared and analyzed for ERK, Akt, IKK, JNK1 and MK2 activity as previously described (Janes et al., 2003). Briefly, lysates were incubated with protein A or G microtiter wells precoated with anti-kinase antibodies. After washing, an appropriate substrate and [ $\gamma$ - $^{32}$ P]ATP was added to the plate to initiate an in vitro phosphorylation reaction. Following termination of the reaction, a fraction of the reaction mix was transferred to a phosphocellulose filter plate and washed to remove free  $^{32}$ P. Protein concentrations of clarified extracts were determined with a bicinchoninic acid assay (Pierce). All activity measurements were adjusted for the specific activation of [ $\gamma$ - $^{32}$ P]ATP and normalized to the total protein content of the sample according to the following calculation:

$$x_t^i = \frac{R_f S_f (CPU_t^i - Bl)}{P_t}$$

where  $x$ =sample value at treatment  $i$  and time point  $t$ ;  $R_f$ =radioactivity decay factor;  $S_f$ =protein scale factor;  $CPU$ =radioactivity of the sample,  $Bl$ =blank (in CPU); and  $P$ =protein concentration (mg/ml). Relative and fold activation are normalized to different baseline (0 minute) activities:

$$\text{Relative activation} = \frac{x_t^i}{x_{0\text{min}}^i}; \text{Fold activation} = \frac{x_t^i}{x_{0\text{min}}^i}$$

where  $x(0\text{A}dv/0\text{min})$  = the zero-minute time point in uninfected cells.

### Western blots

For determination of Akt substrate activity, 50  $\mu$ g of protein lysate from 12 hour Akt activity experiment was resuspended in 40  $\mu$ l sample buffer [62.5 mM Tris-HCl (pH 6.8), 2% SDS, 10% glycerol, 100 mM DTT, 0.01% bromophenol blue]. Samples were boiled for 5 minutes, resolved on a 10% polyacrylamide gel, and transferred to polyvinylidene difluoride (Biorad). Membranes were blocked with 5% nonfat milk in 20 mM Tris-HCl (pH 7.5), 137 mM NaCl, 0.1% Tween-20, and probed with anti-phospho-GSK-3 $\alpha/\beta$  (1:1000; Cell Signaling) or anti-phospho-(Ser/Thr) Akt substrate (1:1000; Cell Signaling). The membranes were then probed with horseradish-peroxidase-conjugated anti-mouse or anti-rabbit secondary antibody (Amersham Pharmacia Biotech) at 1:5000 dilution and visualized by enhanced chemiluminescence (Amersham Pharmacia Biotech) on a Kodak Image

Station (Perkin Elmer). Primary antibodies were removed with stripping buffer [2% SDS, 62.5 mM Tris-HCl (pH 6.8), 100 mM 2-mercaptoethanol].

### Statistical analysis

For comparing two individual means, a Student's  $t$ -test was used. For comparing differences in means on a western blot across multiple blots, a paired Student's  $t$ -test was used. A Pearson's correlation coefficient was calculated to assess linear correlation. For comparing two time courses, a two-way analysis of variance (ANOVA) was used. The sigmoid function was defined as:

$$y = \frac{\text{base} + \text{max}}{1 + \exp\left(\frac{x_{\text{half}} - x}{T_s}\right)}$$

where  $y$ =percent viability,  $x$ =normalized Akt activity or level of phosphorylation,  $\text{base}$ =baseline percent viability,  $\text{max}$ =maximum increase in percent viability,  $x_{\text{half}}$ = $x$  value at which  $y$  is at  $(\text{base} + \text{max})/2$  and  $T_s$ =transition steepness. (Note that smaller  $T_s$  causes a faster rise.) The sigmoid function was fit to data using Igor Pro Graphing software (WaveMetrics).  $\text{Base}$  and  $\text{max}$  values were held constant at 20% and 65%, respectively. The Levenberg-Marquardt non-linear least-squares fitting algorithm was used to search for values of  $x_{\text{half}}$  and  $\text{rate}$  that minimize chi-square. 90% confidence interval for sigmoid curve fit was calculated using support plane analysis (Lakowicz, 1999).

This work was partially supported by the NSF ERC Biotechnology Process Engineering Center (L.G.G.), along with the NIGMS Cell Decision Processes Center and the DoD Institute for Collaborative Biotechnologies (D.A.L.), the American Cancer Society (K.A.J.), and the NIGMS Biotechnology Training Program (K.M.-J.). Technical input and assistance from John Albeck and Nathan Tedford was also greatly helpful.

### References

- Aggarwal, B. B. (2003). Signalling pathways of the TNF superfamily: a double-edged sword. *Nat. Rev. Immunol.* **3**, 745-756.
- Armeanu, S., Lauer, U. M., Smirnow, I., Schenk, M., Weiss, T. S., Gregor, M. and Bitzer, M. (2003). Adenoviral gene transfer of tumor necrosis factor-related apoptosis-inducing ligand overcomes an impaired response of hepatoma cells but causes severe apoptosis in primary human hepatocytes. *Cancer Res.* **63**, 2369-2372.
- Beaulieu, J. M., Sotnikova, T. D., Marion, S., Lefkowitz, R. J., Gainetdinov, R. R. and Caron, M. G. (2005). An Akt/beta-arrestin 2/PP2A signaling complex mediates dopaminergic neurotransmission and behavior. *Cell* **122**, 261-273.
- Beg, A. A. and Baltimore, D. (1996). An essential role for NF-kappaB in preventing TNF-alpha-induced cell death. *Science* **274**, 782-784.
- Benedict, C. A., Norris, P. S., Prigozy, T. I., Bodmer, J. L., Mahr, J. A., Garnett, C. T., Martinon, F., Tschopp, J., Gooding, L. R. and Ware, C. F. (2001). Three adenovirus E3 proteins cooperate to evade apoptosis by tumor necrosis factor-related apoptosis-inducing ligand receptor-1 and -2. *J. Biol. Chem.* **276**, 3270-3278.
- Borgland, S. L., Bowen, G. P., Wong, N. C., Libermann, T. A. and Muruve, D. A. (2000). Adenovirus vector-induced expression of the C-X-C chemokine IP-10 is mediated through capsid-dependent activation of NF-kappaB. *J. Virol.* **74**, 3941-3947.
- Bowen, G. P., Borgland, S. L., Lam, M., Libermann, T. A., Wong, N. C. and Muruve, D. A. (2002). Adenovirus vector-induced inflammation: capsid-dependent induction of the C-C chemokine RANTES requires NF-kappa B. *Hum. Gene Ther.* **13**, 367-379.
- Bruder, J. T. and Kovesdi, I. (1997). Adenovirus infection stimulates the Raf/MAPK signaling pathway and induces interleukin-8 expression. *J. Virol.* **71**, 398-404.
- Cowan, K. J. and Storey, K. B. (2003). Mitogen-activated protein kinases: new signaling pathways functioning in cellular responses to environmental stress. *J. Exp. Biol.* **206**, 1107-1115.
- Cross, D. A., Alessi, D. R., Cohen, P., Andjelkovich, M. and Hemmings, B. A. (1995). Inhibition of glycogen synthase kinase-3 by insulin mediated by protein kinase B. *Nature* **378**, 785-789.
- Davies, S. P., Reddy, H., Caivano, M. and Cohen, P. (2000). Specificity and mechanism of action of some commonly used protein kinase inhibitors. *Biochem. J.* **351**, 95-105.
- Duerksen-Hughes, P., Wold, W. S. and Gooding, L. R. (1989). Adenovirus E1A renders infected cells sensitive to cytolysis by tumor necrosis factor. *J. Immunol.* **143**, 4193-4200.
- Elkon, K. B., Liu, C. C., Gall, J. G., Trevejo, J., Marino, M. W., Abrahamsen, K. A., Song, X., Zhou, J. L., Old, L. J., Crystal, R. G. et al. (1997). Tumor necrosis factor alpha plays a central role in immune-mediated clearance of adenoviral vectors. *Proc. Natl. Acad. Sci. USA* **94**, 9814-9819.
- Flaherty, D. M., Hinde, S. L., Monick, M. M., Powers, L. S., Bradford, M. A., Yarovinsky, T. and Hunninghake, G. W. (2004). Adenovirus vectors activate survival pathways in lung epithelial cells. *Am. J. Physiol. Lung Cell Mol. Physiol.* **287**, L393-L401.
- Fransen, L., Van der Heyden, J., Ruyschaert, R. and Fiers, W. (1986). Recombinant tumor necrosis factor: its effect and its synergism with interferon-gamma on a variety of normal and transformed human cell lines. *Eur. J. Cancer Clin. Oncol.* **22**, 419-426.

- Fulda, S. and Debatin, K. M. (2002). IFN $\gamma$  sensitizes for apoptosis by upregulating caspase-8 expression through the Stat1 pathway. *Oncogene* **21**, 2295-2308.
- Gao, T., Furnari, F. and Newton, A. C. (2005). PHLPP: a phosphatase that directly dephosphorylates Akt, promotes apoptosis, and suppresses tumor growth. *Mol. Cell* **18**, 13-24.
- Garcia-Lloret, M. I., Yui, J., Winkler-Lowen, B. and Guilbert, L. J. (1996). Epidermal growth factor inhibits cytokine-induced apoptosis of primary human trophoblasts. *J. Cell Physiol.* **167**, 324-332.
- Gaudet, S., Janes, K. A., Albeck, J. G., Pace, E. A., Lauffenburger, D. A. and Sorger, P. K. (2005). A compendium of signals and responses triggered by prodeath and prosurvival cytokines. *Mol. Cell Proteomics* **4**, 1569-1590.
- Goldbeter, A. and Koshland, D. E., Jr (1984). Ultrasensitivity in biochemical systems controlled by covalent modification. Interplay between zero-order and multistep effects. *J. Biol. Chem.* **259**, 14441-14447.
- Goldsbey, R. A., Kindt, T. J. and Osborne, B. A. (2000). *Kuby Immunology*. New York: W. H. Freeman.
- Griffith, T. S., Anderson, R. D., Davidson, B. L., Williams, R. D. and Ratliff, T. L. (2000). Adenoviral-mediated transfer of the TNF-related apoptosis-inducing ligand/Apo-2 ligand gene induces tumor cell apoptosis. *J. Immunol.* **165**, 2886-2894.
- Hemmings, B. A., Resink, T. J. and Cohen, P. (1982). Reconstitution of a Mg-ATP-dependent protein phosphatase and its activation through a phosphorylation mechanism. *FEBS Lett.* **150**, 319-324.
- Hersey, P. and Zhang, X. D. (2003). Overcoming resistance of cancer cells to apoptosis. *J. Cell Physiol.* **196**, 9-18.
- Hoefflich, K. P., Luo, J., Rubie, E. A., Tsao, M. S., Jin, O. and Woodgett, J. R. (2000). Requirement for glycogen synthase kinase-3 $\beta$  in cell survival and NF-kappaB activation. *Nature* **406**, 86-90.
- Hua, F., Cornejo, M. G., Cardone, M. H., Stokes, C. L. and Lauffenburger, D. A. (2005). Effects of Bcl-2 levels on Fas signaling-induced caspase-3 activation: molecular genetic tests of computational model predictions. *J. Immunol.* **175**, 985-995.
- Janes, K. A., Albeck, J. G., Peng, L. X., Sorger, P. K., Lauffenburger, D. A. and Yaffe, M. B. (2003). A high-throughput quantitative multiplex kinase assay for monitoring information flow in signaling networks: application to sepsis-apoptosis. *Mol. Cell Proteomics* **2**, 463-473.
- Janes, K. A., Kelly, J. R., Gaudet, S., Albeck, J. G., Sorger, P. K. and Lauffenburger, D. A. (2004). Cue-signal-response analysis of TNF-induced apoptosis by partial least squares regression of dynamic multivariate data. *J. Comp. Biol.* **11**, 544-561.
- Janes, K. A., Albeck, J. G., Gaudet, S., Sorger, P. K., Lauffenburger, D. A. and Yaffe, M. B. (2005). A systems model of signaling identifies a molecular basis set for cytokine-induced apoptosis. *Science* **310**, 1646-1653.
- Janes, K. A., Gaudet, S., Albeck, J. G., Nielsen, U. B., Lauffenburger, D. A. and Sorger, P. K. (2006). The response of human epithelial cells to TNF involves an inducible autocrine cascade. *Cell* **124**, 1225-1239.
- Janeway, C. A., Jr and Medzhitov, R. (2002). Innate immune recognition. *Annu. Rev. Immunol.* **20**, 197-216.
- Karin, M. and Ben-Neriah, Y. (2000). Phosphorylation meets ubiquitination: the control of NF-[kappa]B activity. *Annu. Rev. Immunol.* **18**, 621-663.
- Kotlyarov, A., Neisinger, A., Schubert, C., Eckert, R., Birchmeier, C., Volk, H. D. and Gaestel, M. (1999). MAPKAP kinase 2 is essential for LPS-induced TNF-alpha biosynthesis. *Nat. Cell Biol.* **1**, 94-97.
- Kreuz, S., Siegmund, D., Scheurich, P. and Wajant, H. (2001). NF-[kappa]B inducers upregulate cFLIP, a cycloheximide-sensitive inhibitor of death receptor signaling. *Mol. Cell Biol.* **21**, 3964-3973.
- Lakowicz, J. R. (1999). *Principles of Fluorescence Spectroscopy* (2nd edn). New York: Plenum Press.
- Lawlor, M. A. and Alessi, D. R. (2001). PKB/Akt: a key mediator of cell proliferation, survival and insulin responses? *J. Cell Sci.* **114**, 2903-2910.
- Leers, M. P., Kolgen, W., Bjorklund, V., Bergman, T., Tribbick, G., Persson, B., Bjorklund, P., Ramaekers, F. C., Bjorklund, B., Nap, M. et al. (1999). Immunocytochemical detection and mapping of a cytokeratin 18 neo-epitope exposed during early apoptosis. *J. Pathol.* **187**, 567-572.
- Li, J., Yen, C., Liaw, D., Podsypanina, K., Bose, S., Wang, S. I., Puc, J., Miliareis, C., Rodgers, L., McCombie, R. et al. (1997). PTEN, a putative protein tyrosine phosphatase gene mutated in human brain, breast, and prostate cancer. *Science* **275**, 1943-1947.
- Lieber, A., He, C. Y., Meuse, L., Schowalter, D., Kirillova, I., Winther, B. and Kay, M. A. (1997). The role of Kupffer cell activation and viral gene expression in early liver toxicity after infusion of recombinant adenovirus vectors. *J. Virol.* **71**, 8798-8807.
- Lieber, A., He, C. Y., Meuse, L., Himeda, C., Wilson, C. and Kay, M. A. (1998). Inhibition of NF-kappaB activation in combination with bcl-2 expression allows for persistence of first-generation adenovirus vectors in the mouse liver. *J. Virol.* **72**, 9267-9277.
- Lozier, J. N., Csako, G., Mondoro, T. H., Krizek, D. M., Metzger, M. E., Costello, R., Vostal, J. G., Rick, M. E., Donahue, R. E. and Morgan, R. A. (2002). Toxicity of a First-Generation Adenoviral Vector in Rhesus Macaques. *Human Gene Therapy* **13**, 113-124.
- Manning, B. D., Tee, A. R., Logsdon, M. N., Blenis, J. and Cantley, L. C. (2002). Identification of the tuberous sclerosis complex-2 tumor suppressor gene product tuberin as a target of the phosphoinositide 3-kinase/Akt pathway. *Mol. Cell* **10**, 151-162.
- Mittereder, N., March, K. L. and Trapnell, B. C. (1996). Evaluation of the concentration and bioactivity of adenovirus vectors for gene therapy. *J. Virol.* **70**, 7498-7509.
- Mizuguchi, H. and Hayakawa, T. (2004). Targeted adenovirus vectors. *Hum. Gene Ther.* **15**, 1034-1044.
- Morral, N., O'Neal, W. K., Rice, K., Leland, M. M., Piedra, P. A., Aguilar-Cordova, E., Carey, K. D., Beaudet, A. L. and Langston, C. (2002). Lethal Toxicity, Severe Endothelial Injury, and a Threshold Effect with High Doses of an Adenoviral Vector in Baboons. *Human Gene Therapy* **13**, 143-154.
- Muruve, D. A., Barnes, M. J., Stillman, I. E. and Libermann, T. A. (1999). Adenoviral gene therapy leads to rapid induction of multiple chemokines and acute neutrophil-dependent hepatic injury in vivo. *Hum. Gene Ther.* **10**, 965-976.
- Nyberg-Hoffman, C., Shabram, P., Li, W., Giroux, D. and Aguilar-Cordova, E. (1997). Sensitivity and reproducibility in adenoviral infectious titer determination. *Nat. Med.* **3**, 808-811.
- O'Shea, C., Klupsch, K., Choi, S., Bagus, B., Soria, C., Shen, J., McCormick, F. and Stokoe, D. (2005). Adenoviral proteins mimic nutrient/growth signals to activate the mTOR pathway for viral replication. *EMBO J.* **24**, 1211-1221.
- Ozes, O. N., Mayo, L. D., Gustin, J. A., Pfeffer, S. R., Pfeffer, L. M. and Donner, D. B. (1999). NF-kappaB activation by tumour necrosis factor requires the Akt serine-threonine kinase. *Nature* **401**, 82-85.
- Palmer, D. J. and Ng, P. (2005). Helper-dependent adenoviral vectors for gene therapy. *Hum. Gene Ther.* **16**, 1-16.
- Park, C. S., Schneider, I. C. and Haugh, J. M. (2003). Kinetic analysis of platelet-derived growth factor receptor/phosphoinositide 3-kinase/Akt signaling in fibroblasts. *J. Biol. Chem.* **278**, 37064-37072.
- Prem, S. (ed.) (1999). *Adenoviruses: Basic Biology to Gene Therapy*. Austin: R. G. Landes.
- Qian, H., Hausman, D. B., Compton, M. M., Martin, R. J., Della-Fera, M. A., Hartzell, D. L. and Baile, C. A. (2001). TNFalpha induces and insulin inhibits caspase 3-dependent adipocyte apoptosis. *Biochem. Biophys. Res. Commun.* **284**, 1176-1183.
- Rao, L., Debbas, M., Sabbatini, P., Hockenbery, D., Korsmeyer, S. and White, E. (1992). The adenovirus E1A proteins induce apoptosis, which is inhibited by the E1B 19-kDa and Bcl-2 proteins. *Proc. Natl. Acad. Sci. USA* **89**, 7742-7746.
- Raper, S. E., Yudkoff, M., Chirmule, N., Gao, G.-P., Nunes, F., Haskal, Z. J., Furth, E. E., Propert, K. J., Robinson, M. B., Magosin, S. et al. (2002). A Pilot Study of In Vivo Liver-Directed Gene Transfer with an Adenoviral Vector in Partial Ornithine Transcarbamylase Deficiency. *Human Gene Therapy* **13**, 163-175.
- Rasmussen, H., Rasmussen, C., Lempicki, M., Durham, R., Brough, D., King, C. R. and Weichselbaum, R. (2002). TNFerade Biologic: preclinical toxicology of a novel adenovector with a radiation-inducible promoter, carrying the human tumor necrosis factor alpha gene. *Cancer Gene Ther.* **9**, 951-957.
- Remacle-Bonnet, M. M., Garrouste, F. L., Heller, S., Andre, F., Marvaldi, J. L. and Pommier, G. J. (2000). Insulin-like growth factor-I protects colon cancer cells from death factor-induced apoptosis by potentiating tumor necrosis factor alpha-induced mitogen-activated protein kinase and nuclear factor kappaB signaling pathways. *Cancer Res.* **60**, 2007-2017.
- Rogalla, T., Ehrnsperger, M., Preville, X., Kotlyarov, A., Lutsch, G., Ducasse, C., Paul, C., Wieske, M., Arrigo, A. P., Buchner, J. et al. (1999). Regulation of Hsp27 oligomerization, chaperone function, and protective activity against oxidative stress/tumor necrosis factor alpha by phosphorylation. *J. Biol. Chem.* **274**, 18947-18956.
- Romashkova, J. A. and Makarov, S. S. (1999). NF-kappaB is a target of AKT in anti-apoptotic PDGF signalling. *Nature* **401**, 86-90.
- Saito, Y., Swanson, X., Mhashilkar, A. M., Oida, Y., Schrock, R., Branch, C. D., Chada, S., Zumstein, L. and Ramesh, R. (2003). Adenovirus-mediated transfer of the PTEN gene inhibits human colorectal cancer growth in vitro and in vivo. *Gene Ther.* **10**, 1961-1969.
- Sakashita, G., Shima, H., Komatsu, M., Urano, T., Kikuchi, A. and Kikuchi, K. (2003). Regulation of type 1 protein phosphatase/inhibitor-2 complex by glycogen synthase kinase-3 $\beta$  in intact cells. *J. Biochem.* **133**, 165-171.
- Sasagawa, S., Ozaki, Y., Fujita, K. and Kuroda, S. (2005). Prediction and validation of the distinct dynamics of transient and sustained ERK activation. *Nat. Cell Biol.* **7**, 365-373.
- Schaack, J., Bennett, M. L., Colbert, J. D., Torres, A. V., Clayton, G. H., Ornelles, D. and Moorhead, J. (2004). E1A and E1B proteins inhibit inflammation induced by adenovirus. *Proc. Natl. Acad. Sci. USA* **101**, 3124-3129.
- Schnell, M. A., Zhang, Y., Tazelaar, J., Gao, G. P., Yu, C. Q., Qian, R., Chen, S. J., Varnavski, A. N., LeClair, C., Raper, S. E. et al. (2001). Activation of innate immunity in nonhuman primates following intraportal administration of adenoviral vectors. *Mol. Ther.* **3**, 708-722.
- Shaulian, E. and Karin, M. (2002). AP-1 as a regulator of cell life and death. *Nat. Cell Biol.* **4**, E131-E136.
- Stupack, D. G. and Cheresch, D. A. (2002). Get a ligand, get a life: integrins, signaling and cell survival. *J. Cell Sci.* **115**, 3729-3738.
- Tamanini, A., Rolfini, R., Nicolis, E., Melotti, P. and Cabrini, G. (2003). MAP kinases and NF-[kappa]B collaborate to induce ICAM-1 gene expression in the early phase of adenovirus infection. *Virology* **307**, 228-242.
- Tanji, C., Yamamoto, H., Yorioka, N., Kohno, N., Kikuchi, K. and Kikuchi, A. (2002). A-kinase anchoring protein AKAP220 binds to glycogen synthase kinase-3 $\beta$  (GSK-3 $\beta$ ) and mediates protein kinase A-dependent inhibition of GSK-3 $\beta$ . *J. Biol. Chem.* **277**, 36955-36961.
- Tauber, B. and Dobner, T. (2001). Molecular regulation and biological function of adenovirus early genes: the E4 ORFs. *Gene* **278**, 1-23.
- Thomas, C. E., Ehrhardt, A. and Kay, M. A. (2003). Progress and problems with the use of viral vectors for gene therapy. *Nat. Rev. Genet.* **4**, 346-358.

- Tibbles, L. A., Spurrell, J. C., Bowen, G. P., Liu, Q., Lam, M., Zaiss, A. K., Robbins, S. M., Hollenberg, M. D., Wickham, T. J. and Muruve, D. A. (2002). Activation of p38 and ERK signaling during adenovirus vector cell entry lead to expression of the C-X-C chemokine IP-10. *J. Virol.* **76**, 1559-1568.
- Van Antwerp, D. J., Martin, S. J., Kafri, T., Green, D. R. and Verma, I. M. (1996). Suppression of TNF-alpha-induced apoptosis by NF-kappaB. *Science* **274**, 787-789.
- Varga, C. M., Hong, K. and Lauffenburger, D. A. (2001). Quantitative analysis of synthetic gene delivery vector design properties. *Mol. Ther.* **4**, 438-446.
- Ventura, J. J., Cogswell, P., Flavell, R. A., Baldwin, A. S., Jr and Davis, R. J. (2004). JNK potentiates TNF-stimulated necrosis by increasing the production of cytotoxic reactive oxygen species. *Genes Dev.* **18**, 2905-2915.
- Verma, I. M. and Weitzman, M. D. (2005). Gene therapy: twenty-first century medicine. *Annu. Rev. Biochem.* **74**, 711-738.
- Voelkel-Johnson, C., King, D. L. and Norris, J. S. (2002). Resistance of prostate cancer cells to soluble TNF-related apoptosis-inducing ligand (TRAIL/Apo2L) can be overcome by doxorubicin or adenoviral delivery of full-length TRAIL. *Cancer Gene Ther.* **9**, 164-172.
- Wajant, H., Pfizenmaier, K. and Scheurich, P. (2003). Tumor necrosis factor signaling. *Cell Death Differ.* **10**, 45-65.
- Wang, C. Y., Mayo, M. W. and Baldwin, A. S., Jr (1996). TNF- and cancer therapy-induced apoptosis: potentiation by inhibition of NF-kappaB. *Science* **274**, 784-787.
- Zhang, F., Cheng, J., Hackett, N. R., Lam, G., Shido, K., Pergolizzi, R., Jin, D. K., Crystal, R. G. and Rafii, S. (2004). Adenovirus E4 gene promotes selective endothelial cell survival and angiogenesis via activation of the vascular endothelial-cadherin/Akt signaling pathway. *J. Biol. Chem.* **279**, 11760-11766.
- Zhang, H. G., Zhou, T., Yang, P., Edwards, C. K., 3rd, Curiel, D. T. and Mountz, J. D. (1998). Inhibition of tumor necrosis factor alpha decreases inflammation and prolongs adenovirus gene expression in lung and liver. *Hum. Gene Ther.* **9**, 1875-1884.
- Zhang, H. G., Xie, J., Xu, L., Yang, P., Xu, X., Sun, S., Wang, Y., Curiel, D. T., Hsu, H. C. and Mountz, J. D. (2002). Hepatic DR5 induces apoptosis and limits adenovirus gene therapy product expression in the liver. *J. Virol.* **76**, 5692-5700.
- Zhang, Y., Chirmule, N., Gao, G. P., Qian, R., Croyle, M., Joshi, B., Tazelaar, J. and Wilson, J. M. (2001). Acute cytokine response to systemic adenoviral vectors in mice is mediated by dendritic cells and macrophages. *Mol. Ther.* **3**, 697-707.